Bioorg. Med. Chem. Lett. 46 (2021) 128171

Contents lists available at ScienceDirect

Bioorganic & Medicinal Chemistry Letters

journal homepage: www.elsevier.com/locate/bmcl

Synthesis and biological activity of conformationally restricted indole-based inhibitors of neurotropic alphavirus replication: Generation of a three-dimensional pharmacophore

Scott J. Barraza [b], Janice A. Sindac [b], Craig J. Dobry [c], Philip C. Delekta [c], Pil H. Lee [a,b], David J. Miller [c], Scott D. Larsen [a,b,*]

[a] Vahlteich Medicinal Chemistry Core, University of Michigan, Ann Arbor, MI 48109, United States
[b] Department of Medicinal Chemistry, College of Pharmacy, University of Michigan, Ann Arbor, MI 48109, United States
[c] Departments of Internal Medicine and Microbiology and Immunology, University of Michigan, Ann Arbor, MI 48109, United States

ARTICLE INFO

Keywords:
Neurotropic alphavirus
Antiviral
Pharmacophore
Conformationally restricted
Western equine encephalitis virus

ABSTRACT

We have previously reported the development of indole-based CNS-active antivirals for the treatment of neurotropic alphavirus infection, but further optimization is impeded by a lack of knowledge of the molecular target and binding site. Herein we describe the design, synthesis and evaluation of a series of conformationally restricted analogues with the dual objectives of improving potency/selectivity and identifying the most bioactive conformation. Although this campaign was only modestly successful at improving potency, the sharply defined SAR of the rigid analogs enabled the definition of a three-dimensional pharmacophore, which we believe will be of value in further analog design and virtual screening for alternative antiviral leads.

Neurotropic alphaviruses are NIAID Category B Priority pathogens that infect the central nervous system (CNS) and have the potential to cause severe and debilitating disease in humans and animals.[1] Among these, the mosquito-borne equine encephalitis viruses (Eastern, Western, and Venezuelan) are endemic to the Americas and constitute an emergent public health risk due to the potential for human mortality[2] and neurological damage,[3–5] in addition to disruption of agriculture.[6–7] Despite this risk, prophylactic therapies are inadequate; current vaccines lack wide availability and exhibit limited efficacy in humans,[8–9] and recent vaccine candidates have demonstrated protection in animal models only.[10–13] Options for treating infection with small molecule drugs are similarly minimal and are unable to compensate for vaccine deficiencies. For example, the efficacy of the current standard of treatment, ribavirin, is constrained by poor CNS exposure.[14–16] Remarkably, equine encephalitis viruses have received scant historical attention to address these shortcomings.[17] Only a handful of reports have been published in recent years detailing the discovery of drug-like small molecules[18–20] and natural products,[21–22] so there remains an urgent need to identify and develop effective therapies that can intercede with infection.

We have previously reported the discovery[23] and optimization[24–25] of indole-based alphavirus RNA replication inhibitors, e.g. **1** and **2** (Figure 1), and, more recently, anthranilamide-based inhibitors possessing improved pharmacokinetic properties.[26] Unfortunately, the molecular target remains elusive – a consequence of the phenotypic nature of our primary antiviral assays – and thus the architecture of the binding site that could guide design of more potent inhibitors is unknown. An approach that is often effective in such a scenario is the synthesis and evaluation of rigid analogues.[27–30] Of the multiple conformations that a drug can adopt, only a small subset are expected to have maximal activity if the binding site is well defined.[31] It can therefore be informative to restrict lead molecules into specific conformations in an effort to pinpoint the most active ones.[32] In addition to the obvious benefit of potentially defining a 3-dimensional (3D) pharmacophore, this strategy can also improve both potency and selectivity versus off-target effects.[33–35]

In the present work, we thus pursued two central objectives: (1) to conformationally restrict rotatable bonds in our leads **1** and **2**, and (2) to develop a 3D pharmacophore model based on the resulting SAR that could expedite future drug design. Toward this end, we describe three different approaches to conformational restriction: 1) replacement of small functionality with sterically demanding functionality; 2) bridging

* Corresponding author.
E-mail address: sdlarsen@med.umich.edu (S.D. Larsen).

https://doi.org/10.1016/j.bmcl.2021.128171
Received 15 February 2021; Received in revised form 26 May 2021; Accepted 30 May 2021
Available online 15 June 2021

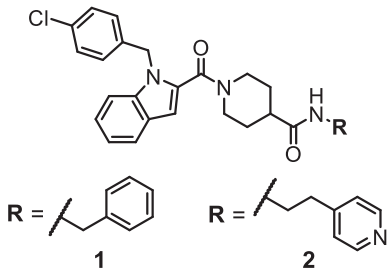

Fig. 1. Indole-based alphavirus replication inhibitor leads.

of nonadjacent atoms; and 3) freezing of ring conformations. We also strove to minimize the number of additional atoms used in locking conformations because higher molecular weight could impede CNS permeability.

Analogs were synthesized according to one of two general procedures (Scheme 1). In all cases where chiral centers were present, the analogs were prepared and tested as racemates. General Procedure A was used to incorporate methyl groups onto the indole and to modify the benzyl group of lead **1**. *N*-(4-Chlorobenzyl)indole-2-carboxylic acids **30a–c**[36] were condensed with ethyl isonipecotate or ethyl nipecotate and the respective esters were subsequently hydrolyzed to afford carboxylic acid intermediates **31a–c**. These acids were condensed with a variety of amines (see Supporting Information) to produce analogs **3** – **16** (Tables 1 and 2).

Alternatively, General Procedure B was employed to explore changes to the piperidine and amide moieties of lead **2** (Scheme 1). Piperidines, piperazines, and bicyclic amines were functionalized through a variety of reactions to afford intermediates with the general structure **34** (Scheme 2 and Supp. Info). Following deprotection, these intermediates were condensed with *N*-(4-chlorobenzyl)indole-2-carboxylic acid **30a** to afford analogs **17– 29** (Table 3).

The majority of intermediates of general structure **34** were amides and as such were prepared by condensation of an amine with a carboxylic acid followed by acid-promoted Boc-deprotection (e.g. **37** and **42**, Scheme 2 ; for others, see SI). Urea **40** was prepared by condensation of two different amines with phosgene and was likewise deprotected. *N*-Tosyl-protected spirocyclic amino acid **43**[37–39] was similarly condensed with 4-(2-aminoethyl)-pyridine **39** but proved challenging to deprotect. Samarium (II) iodide either failed to remove the tosyl under neutral conditions or afforded reductive cleavage of the amide in the presence of tertiary amines,[40,41] and other methods[42,43] were similarly unsuccessful. Only sodium naphthalenide cleanly cleaved the S—N bond to afford amine **44**.

Distinct from the other intermediates, alkenes **47** and **48** were synthesized via a traditional Wittig reaction and the Schlosser modification thereof,[44] respectively, from *N*-boc-4-formylpiperidine **45** and phosphonium bromide **46**[45] (Scheme 2). Although a large number of highly E- and Z-selective olefinations exist,[46] this divergent approach allowed for convenient and rapid access to both alkenes from the same reactants. All new analogues were evaluated for antiviral activity in a phenotypic cell-based assay against the WEEV genome replicon as previously described.[25] Analogues were also tested for cytotoxicity under similar conditions using a colorimetric MTT assay. The data appear in Tables 1-4.

As noted earlier, definition of a 3D pharmacophore was our primary goal through the evaluation of conformationally-restricted analogs. Our initial efforts focused on the restriction of the indole substituents of the lead **1**[25] (Table 1). Utilizing a non-covalent steric approach, two compounds were designed on the notion that strategically placed methyl groups would impede bond rotations of adjacent sidechains with minimal impact on molecular weight. Both the 7-methylindole **3** and the 3-methylindole **4** possessed substantially reduced potency, indicating that the methyl groups may be preventing rotatable access of the *N*-benzyl group and the 2-carboxamide to active conformations.

We next turned to restricting the flexibility of the *N*-benzyl amide on

Table 1
Modification of the indole of **1**.

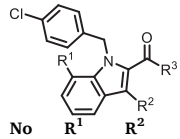

No	R^1	R^2	R^3	IC_{50} (μM)[a]	CC_{50} (μM)[b]
1[25]	H	H	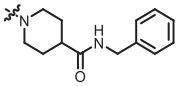	15.6 ± 1.8	>100
3	CH_3	H	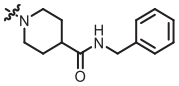	61 ± 39	>100
4	H	CH_3	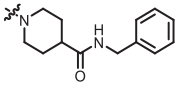	>100	>100

[a]Inhibition of luciferase expression in WEEV replicon assay. [b]Cell viability determined by the MTT reduction assay. Values are mean of at least n = 3 independent experiments.

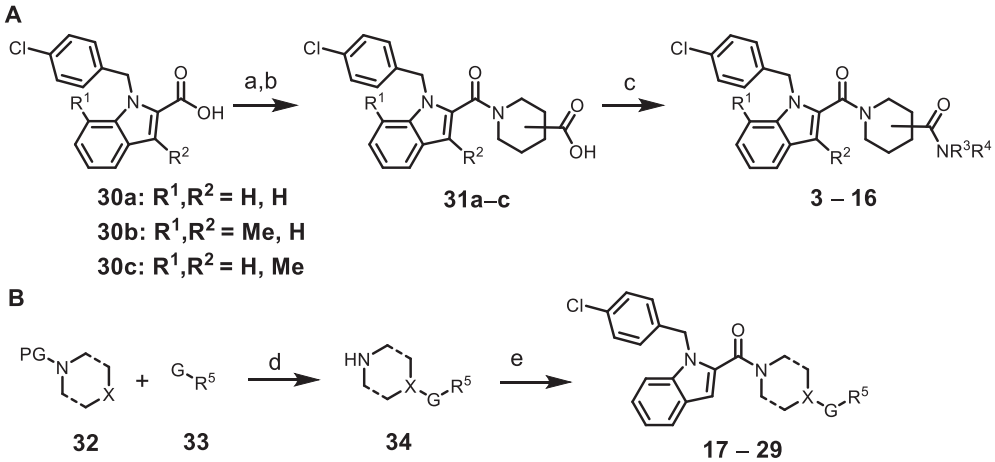

Scheme 1. General Procedure A reagents and conditions: (a) ethyl isonipecotate or ethyl nipecotate, EDC, HOBT, TEA, DCM, r.t.; (b) NaOH, H_2O, THF, r.t.; (c) R^3R^4NH, EDC, HOBT, TEA, DCM, r.t.; General Procedure B reagents and conditions: (d) various reactions – see Scheme 2 and SI; (e) **30a**, EDC, TEA, HOBT, DCM, r.t. PG = protecting group; G = reactive group.

Table 2
Modification of the benzyl amide of **1**.

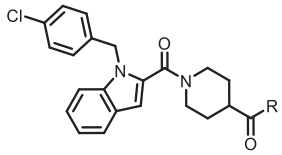

No	R	IC_{50} (μM)[a]	CC_{50} (μM)[b]
1[25]	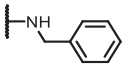	15.6 ± 1.8	>100
5[c]	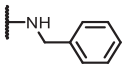	30.6 ± 7.3	>100
6	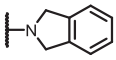	>100	>100
7	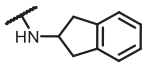	>100	>100
8	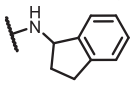	>100	>100
9	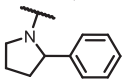	>100	>100
10	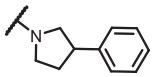	>100	>100
11	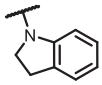	>100	>100
12	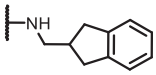	0.53 ± 0.04	>100
13	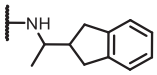	1.7 ± 0.1	>100
14	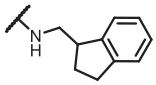	7.1 ± 0.9	>100
15[25]	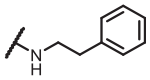	15.2 ± 4.7	62 ± 13
16	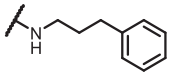	>100	>50

[a]Inhibition of luciferase expression in WEEV replicon assay. [b]Cell viability determined by the MTT reduction assay. Values are mean of at least n = 3 independent experiments. [c]Based on nipecotic acid central ring (racemate).[25]

the isonipecotic acid frame of **1** (Table 2). Previously prepared analogs[25] **5** and **15** are included in the table for comparison. Remarkably, the majority of new analogs (**6 – 11**) exhibited no activity whatsoever, suggesting that the binding pocket for the *N*-benzyl amide is well defined and intolerant of many rigid conformations. One compound (**12**), however, proved to possess markedly better potency than all others in this series, which we do not believe can be attributed to simple increased lipophilicity or chain extension because analogs of similar ClogP (**14**) and length (**15**[25] and **16**) were less potent (Table 2). Interestingly, the racemic methyl analog **13** was also quite active; however its lower potency relative to **12** is further evidence that the amide binding site is well defined and not tolerant of even modest additional bulk or altered conformation. Importantly, the increased potency of **12** has apparently been achieved without a commensurate increase in cytotoxicity vs **1.** Finally, the dramatic loss of potency of analogs **7** and **8**, each a single methylene shorter than the corresponding active analogs **12** and **14**, respectively, suggests that some degree of flexibility is required to engage the binding site. Overall, the results in Table 2 are consistent with an amide binding pocket in the unknown molecular target that is very well defined and discriminating.

Our attention then turned towards the central piperidine ring and the piperidine-4-carboxamide. Compound **2**[24] was employed as the lead for this series due to its equipotency with **12** and greater ease of analog synthesis. Biological results are summarized in Table 3. The carboxamide imparts significant conformational bias to the linker between the piperidine and the pyridine, so we initially explored replacing it with E or Z olefins **17** and **18**, respectively, which are conformationally locked bioisosteres for the two possible rotamers of the carboxamide.[47] Remarkably, both analogs lost all activity, indicating that the caboxamide itself is likely making at least one key binding interaction. To explore this further, inverse amide **19** and shifted amide **20** were prepared, each proving to be over 30-fold less active than **2**. This supported that a carboxamide bound directly to the piperidine 4-carbon through the carbonyl is a critical part of the pharmacophore. We therefore retained this motif through the remainder of our investigation.

Urea analog **21** and unsaturated amide **22** were examined next, each of which retained all of the atoms of the carboxamide and its position relative to the piperidine, but would be expected to have some minor conformational differences. The simple unsaturated amide retained more activity than the urea, but still lost nearly 10-fold potency. Methyl analogs **23** and **24** were particularly informative. While the previously prepared *N*-methyl analog **24**[24] only lost 2-fold potency, suggesting that the N—H is not functioning as a hydrogen bond donor, the new α-methyl analog **23** lost all activity, indicating that the carbonyl likely plays a much more significant role. The α-methyl group is either occluding the amide carbonyl from binding (sterically or conformationally) or is impeding favorable chair conformations of the piperidine. Finally, since we had shown with **24** that the N—H was not critical for activity, we prepared the highly rigid bicyclic analog **25**. This analog lost most potency, obviously indicating that it is not locked in the optimal conformation. Collectively, the results for **17** – **25** highlight the importance of a sterically unhindered and flexible carboxamide to the pharmacophore.

For the next three analogs **26** – **28**, we retained the "flexible" carboxamide moiety in the linker, and focused on freezing the conformational mobility of the piperidine ring. While the *exo*-bicycle **26** and the spirocycle **28** lost over 20-fold potency, the tricyclic analog **27** retained almost all of the potency of lead **2**, suggesting that the locked equatorial-equatorial relationship between the 1- and 4-substituents may reflect the unknown bioactive conformation, Unfortunately, no activity improvement was realized by this conformational restraint.

Conversely, we examined an azapane analog **29** that we expected would be more flexible than piperidine **2** but about the same overall length. Interestingly, this compound was equally potent with the lead despite being a racemate. Depending on the eudismic ratio (not determined), the active enantiomer could potentially be two-fold more active, marking this compound as the most active compound to-date in the WEEV replicon assay. The simplest explanation for this positive result is that a larger population of azapane conformers are available that are favorable to binding than are available to the piperidine.

The replicon activity of azapane **29** was confirmed in an antiviral assay in FMV-infected BE(2)-C cells. At 5 μM, **29** demonstrated a nearly two-fold improvement in infected cell viability (36.1 ± 4.0% versus negative control 19.6 ± 4.0%), similar to the two-fold enhancement observed for lead **2** at 25 μM. At higher concentration improvement was more modest (22.9 ± 4.9% cell viability at 25 μM), possibly due to concentration-dependent cytotoxicity.

The primary objective of this work was to establish a 3D pharmacophore model that could facilitate future optimization and enable virtual screening to identify alternative templates. We first noted that a number of small changes in the structure resulted in large differences in biological activity, suggesting that an "activity cliff" analysis[48] could be useful for identifying key pharmacophoric elements. Employing DataWarrior[49], we identified pairs of compounds exhibiting both high 2D structural similarity and divergent potency and ranked them according to structure activity landscape index (SALI)[50] scores (Table S1 in

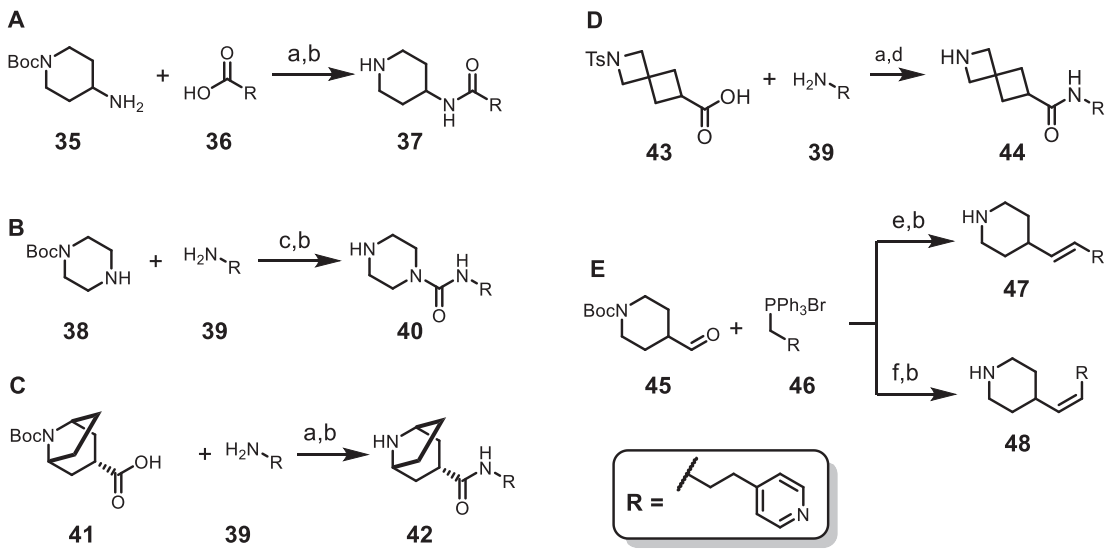

Scheme 2. Reagents and conditions: (a) EDC, HOBT, Et_3N, DCM, r.t.; (b) HCl, dioxane, r.t.; (c) $COCl_2$, Et_3N, toluene, DCM, 0 °C; (d) Na^0, naphthalene, THF, r.t.; (e) PhLi, *t*-BuOH, LiBr, THF, −78 °C − r.t.; (f) *n*-BuLi, THF, r.t.

Supporting Information). Based on the pairs having the greatest SALI values, there appear to be three pharmacophoric features most sensitive to structural changes: the distance between the terminal aryl group and the piperidine (e.g. **16** vs **15**, **12** vs **6**, **12** vs **14**), the flexibility of the linker to the terminal aryl group (**7** vs **12**, **8** vs **14**) and the piperidine-4-carboxamide carbonyl on the piperidine (**2** vs **23**, **2** vs **17**/**18**, **2** vs **20**, **2** vs **19**).

In order to generate a hypothetical 3D pharmacophore, we used the Pharmacophore Elucidation tool in MOE 2019.0102.[51] The approach for Pharmacophore Elucidation is to exhaustively search for all pharmacophore queries (arrangements of molecular features such as aromatic rinds, hydrophobic groups, hydrogen bond acceptors/donors, etc.) that induce good overlay of most of the active molecules and separate actives from inactives. It was assumed that all or most of the active compounds bind to the same biological target in a similar way and can therefore be overlaid.

"Active" compounds were defined as those with $IC_{50} < 5$ μM, affording a set of 7 actives and 22 inactives. These sets were used to generate a collection of pharmacophore queries such that all or most of the active compounds satisfy the queries. The generated queries were then scored by the accuracy of separating actives and inactives. The overall accuracy = m/N where N is the number of compounds in the input database and m is the sum of the number of actives that match the query and the number of inactives that do not match the query. Queries were also scored by degree of overlap of the actives with the pharmacophoric features. The overlap is between 0 and n where n is the number of actives. The larger the overlap the better the alignment. The overlap is calculated by the heavy atom root mean square deviation among the aligned compounds.

The program generated a database of 8850 queries from our analogue set. The output database contained the conformations of the high scoring alignment induced by the query, features of each query, the number of actives that match the query, the score of the alignment, the accuracy of the query in separating actives and inactives, the accuracies of the query in matching the actives/inactives, etc. The queries were sorted by the accuracies, and the top queries were examined for the alignment of actives (see Table S2 in Supporting Information for the top 10 queries.) One query (H H H a a) was selected as the best on the aggregate basis of accuracy, overlap, and agreement with the activity cliff analysis. The selected query has 5 features: 3 hydrophobic groups and 2 hydrogen bond acceptors (defined as the postulated locations of potential hydrogen bond donors).

The overall accuracy of this query is 0.93 out of 1.0; all the actives except for one (**27**) match this query, all of the inactives except for one do not match this query, and the overlap of the actives is 5.22 out of 6.0. The alignment of the six most active compounds overlaid on top of the pharmacophoric query is shown in Figure 2. This query contains the terminal hydrophobic group, which is consistent with the activity cliff analysis above. It also contains two hydrogen bond acceptors, one of which is the piperidine-4-carboxamide which was also shown to be important in the activity cliff analysis. A detailed description of how the pharmacophore elucidation was performed is provided in the Supporting Information.

In conclusion, we have explored a variety of conformationally restricted analogs of our WEEV antiviral leads **1** and **2**, with several objectives in mind: 1) improving antiviral potency; 2) increasing selectivity vs off-targets that could reduce cytotoxicity; and 3) beginning to define a 3D pharmacophore for the unknown molecular target to facilitate future design, including virtual screening to potentially identify new lead chemotypes. Both covalent and non-covalent approaches to restricting rotational freedom were examined. As expected, many rigid analogs completely lost activity, suggesting that the binding site is well defined and highly discriminating based on molecular shape. Significant improvements in antiviral potency were realized with terminal amide analogs of **1** (e.g. **12**) without increasing cytotoxicity, suggesting some improvement in selectivity for the unknown viral target. Modification of the carboxamide and piperidine of more potent lead **2** were less successful at improving potency but helped to identify important pharmacophoric elements. The piperidine ring had little tolerance for conformational rigidity, with only the locked 1,4-diequatorial analog **27** retaining most of the potency of lead **2**. Conversely, increasing flexibility, as in azapane analog **29**, actually improved potency slightly. We applied computational modeling to identify the most important SAR (activity cliffs) and to subsequently define a common pharmacophore which rationalized most of the SAR. Key elements of this pharmacophore include an optimum linker length between the indole and the terminal aromatic group of the amide *N*-substituent, as well as the requirement for a carboxamide with precise placement on the linker and an unhindered carbonyl. We believe this pharmacophore could be useful for designing new compounds and may enable virtual screening to identify novel viral replication inhibitors.

Table 3
Modification of the piperidine amide of **2.**

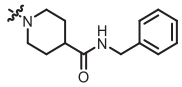

No	R	IC_{50} (μM)[a]	CC_{50} (μM)[b]
2[24]	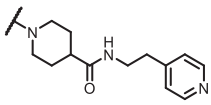	0.53 ± 0.08	65.0
17	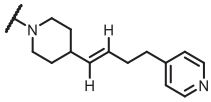	>50	>50
18	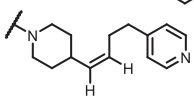	>50	>50
19	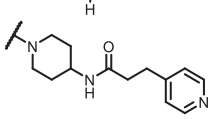	17.6[c]	66.7[c]
20	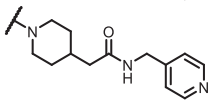	24.7 ± 3.5	77.3
21	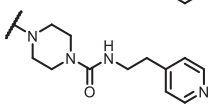	24.4 ± 4.0	78.0
22	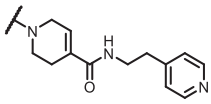	3.9 ± 0.4	74.2
23	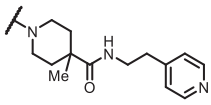	>50	>50
24[24]	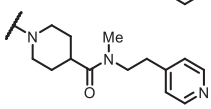	1.6 ± 0.8	47.9
25	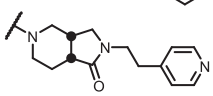	24.4 ± 6.3	61.0
26	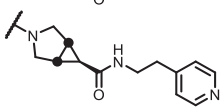	24.6 ± 1.6	>100
27	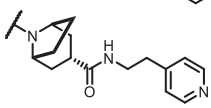	0.96 ± 0.06	50.9
28	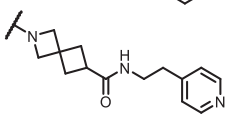	10.9 ± 0.6	56.5
29	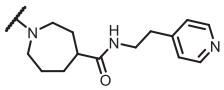	0.49 ± 0.09	41.1

[a]Inhibition of luciferase expression in WEEV replicon assay. [b]Cell viability determined by the MTT reduction assay. Values are mean of at least n = 3 independent experiments. [c]Value is n = 1 experiment.

Declaration of Competing Interest

The authors declare that they have no known competing financial interests or personal relationships that could have appeared to influence the work reported in this paper.

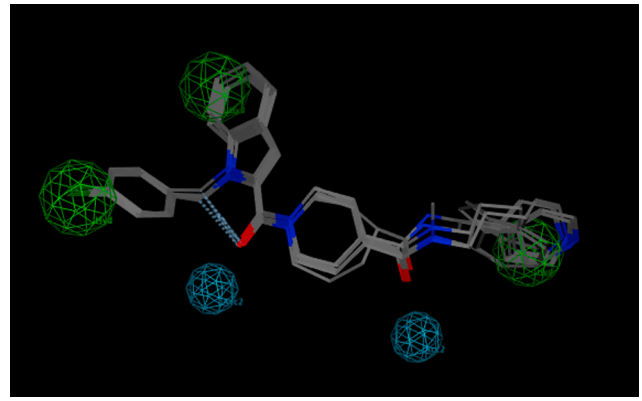

Fig. 2. The overlay of the six active analogs with the pharmacophoric query. Green represents location of hydrophobic groups and cyan indicates hydrogen bond acceptors (represented by optimal location of potential hydrogen bond donors in binding site).

Acknowledgements

This work was supported by an NIH Partnerships for Biodefense Viral Pathogens grant (R01 AI089417, Principal Investigator DJM) and a University of Michigan Rackham Merit Scholarship for SJB.

Appendix A. Supplementary data

Supplementary data to this article can be found online at https://doi.org/10.1016/j.bmcl.2021.128171.

References

1 Smith DR, Schmaljohn CS, Badger C, et al. Comparative pathology study of Venezuelan, eastern, and western equine encephalitis viruses in non-human primates. *Antiviral Res*. 2020;182:104875. https://doi.org/10.1016/j.antiviral.2020.104875.
2 Zacks MA, Paessler S. Encephalitic alphaviruses. *Vet Microbiol*. 2010;140(3-4):281–286.
3 Feemster RF. Equine Encephalitis in Massachusetts. *New Engl J Med*. 1957;257(15):701–704.
4 Deresiewicz RL, Thaler SJ, Hsu L, Zamani AA. Clinical and neuroradiographic manifestations of Eastern equine encephalitis. *New Engl J Med*. 1997;336(26):1867–1874.
5 Bantle CM, Phillips AT, Smeyne RJ, Rocha SM, Olson KE, Tjalkens RB. Infection with mosquito-borne alphavirus induces selective loss of dopaminergic neurons, neuroinflammation and widespread protein aggregation. *NPJ Parkinsons Dis*. 2019;5:20.
6 Rivas F, Diaz LA, Cardenas VM, et al. Epidemic Venezuelan equine encephalitis in La Guajira, Colombia, 1995. *J Infect Dis*. 1997;175(4):828–832.
7 Ehrenkranz, N. J.; Ventura, A. K., Venezuelan Equine Encephalitis Virus Infection in Man. 1974, 9-14.
8 Griffin DE, Shoshkes Reiss C. In: *Neurotropic Viral Infections*. Cambridge: Cambridge University Press; 2008:94–119. https://doi.org/10.1017/CBO9780511541728.009.
9 Steele, K. E. R., D.S.; Glass, P.J.; Hart, M.K.; Ludwig, G.V.; Pratt, W.D.; Parker, M.D.; Smith, J.F., Alphavirus Encephalitides. In Medical Aspects of Biological Warfare, Dembek, Z. F., Ed. Office of the Surgeon General: United States of America, 2007; pp 241-270.
10 Dupuy LC, Richards MJ, Livingston BD, Hannaman D, Schmaljohn CS. A Multiagent Alphavirus DNA Vaccine Delivered by Intramuscular Electroporation Elicits Robust and Durable Virus-Specific Immune Responses in Mice and Rabbits and Completely Protects Mice against Lethal Venezuelan, Western, and Eastern Equine Encephalitis Virus Aerosol Challenges. *J Immunol Res*. 2018;2018:1–15.
11 C.W. Burke J.W. Froude S. Miethe B. Hulseweh M. Hust P.J. Glass Human-Like Neutralizing Antibodies Protect Mice from Aerosol Exposure with Western Equine Encephalitis Virus Viruses 10 4 2018 147/1-147/7.
12 S.-Y. Ko W. Akahata E.S. Yang et al. A virus-like particle vaccine prevents equine encephalitis virus infection in nonhuman primates Sci Transl Med 11 492 2019 eaav3113 10.1126/scitranslmed.aav3113.
13 Stromberg ZR, Fischer W, Bradfute SB, Kubicek-Sutherland JZ, Hraber P. Vaccine Advances against Venezuelan, Eastern, and Western Equine Encephalitis Viruses. *Vaccines (Basel)*. 2020;8(2):273.
14 Colombo G, Lorenzini L, Zironi E, et al. Brain distribution of ribavirin after intranasal administration. *Antiviral Res*. 2011;92(3):408–414.
15 Snell NJC. Ribavirin - current status of a broad spectrum antiviral agent. *Expert Opin Pharmacother*. 2001;2(8):1317–1324.

16 Huggins JW. Prospects for treatment of viral hemorrhagic fevers with ribavirin, a broad-spectrum antiviral drug. *Rev Infect Dis*. 1989;11(Suppl 4):S750–S761.
17 Reichert E, Clase A, Bacetty A, Larsen J. Alphavirus antiviral drug development: scientific gap analysis and prospective research areas. *Biosecur Bioterror*. 2009;7(4):413–427.
18 Madsen C, Hooper I, Lundberg L, et al. Small molecule inhibitors of Ago2 decrease Venezuelan equine encephalitis virus replication. *Antiviral Res*. 2014;112:26–37.
19 Nguyen TH, Haese NN, Madadi N, et al. Studies on Dibenzylamines as Inhibitors of Venezuelan Equine Encephalitis Virus. *ACS Infect Dis*. 2019;5(12):2014–2028.
20 Saikh KU, Morazzani EM, Piper AE, Bakken RR, Glass PJ. A small molecule inhibitor of MyD88 exhibits broad spectrum antiviral activity by up regulation of type I interferon. *Antiviral Res*. 2020;181:104854. https://doi.org/10.1016/j.antiviral.2020.104854.
21 Delekta PC, Raveh A, Larsen MJ, et al. The combined use of alphavirus replicons and pseudoinfectious particles for the discovery of antivirals derived from natural products. *J Biomol Screen*. 2015;20(5):673–680.
22 Sabini MC, Cariddi LN, Escobar FM, et al. Potent inhibition of Western Equine Encephalitis virus by a fraction rich in flavonoids and phenolic acids obtained from Achyrocline satureioides. *Revista Brasileira de Farmacognosia*. 2016;26(5):571–578.
23 Peng W, Peltier D, Larsen M, et al. Identification of thieno[3,2-b]pyrrole derivatives as novel small molecule inhibitors of neurotropic alphaviruses. *J Infect Dis*. 2009;199(7):950–957.
24 Sindac JA, Barraza SJ, Dobry CJ, et al. Optimization of Novel Indole-2-carboxamide Inhibitors of Neurotropic Alphavirus Replication. *J Med Chem*. 2013;56(22):9222–9241.
25 Sindac JA, Yestrepsky BD, Barraza SJ, et al. Novel Inhibitors of Neurotropic Alphavirus Replication That Improve Host Survival in a Mouse Model of Acute Viral Encephalitis. *J Med Chem*. 2012;55(7):3535–3545.
26 Barraza SJ, Delekta PC, Sindac JA, et al. Discovery of anthranilamides as a novel class of inhibitors of neurotropic alphavirus replication. *Bioorg Med Chem*. 2015;23(7):1569–1587.
27 Lemke, T. L. W., D.A., Foye's Principles of Medicinal Chemistry. Sixth ed.; Lippincott Williams and Wilkinds: USA, 2008.
28 Vagner J, Qu H, Hruby VJ. Peptidomimetics, a synthetic tool of drug discovery. *Curr Opin Chem Biol*. 2008;12(3):292–296.
29 Lima LMA, Barreiro EJ. Bioisosterism: A useful strategy for molecular modification and drug design. *Curr Med Chem*. 2005;12(1):23–49.
30 Olesen PH. The use of bioisosteric groups in lead optimization. *Curr Opin Drug Discov Devel*. 2001;4(4):471–478.
31 Taylor RD, Jewsbury PJ, Essex JW. A review of protein-small molecule docking methods. *J Comput Aided Mol Des*. 2002;16(3):151–166.
32 Wermuth, C. G. M., A., The Practice of Medicinal Chemistry. Second ed.; Wermuth, C. G., Ed. Elsevier Inc.: USA, 2003.
33 Dwoskin LP, Crooks PA. Competitive Neuronal Nicotinic Receptor Antagonists: A New Direction for Drug Discovery. *J Pharmacol Exp Ther*. 2001;298(2):395–402.
34 Kazuta Y, Hirano K, Natsume K, et al. Cyclopropane-Based Conformational Restriction of Histamine. (1S,2S)-2-(2-Aminoethyl)-1-(1H-imidazol-4-yl) cyclopropane, a Highly Selective Agonist for the Histamine H3 Receptor, Having a cis-Cyclopropane Structure. *J Med Chem*. 2003;46(10):1980–1988.
35 Willhite CC, Dawson MI. Structure-activity relationships of retinoids in developmental toxicology: IV. Planar cisoid conformational restriction. *Toxicol Appl Pharmacol*. 1990;103(2):324–344.
36 Larsen, S.; Sindac, J.; Barraza, S.; Miller David, J. Arbovirus Inhibitors And Uses Thereof. US 2012/0252807 A1, 2012/03/19, 2012.
37 Radchenko DS, Grygorenko OO, Komarov IV. Synthesis of 2-azaspiro[3.3]heptane-derived amino acids: ornitine and GABA analogues. *Amino Acids*. 2010;39(2):515–521.
38 Radchenko DS, Pavlenko SO, Grygorenko OO, et al. Cyclobutane-Derived Diamines: Synthesis and Molecular Structure. *J Organ Chem*. 2010;75(17):5941–5952.
39 Allinger NL, Tushaus LA. Conformational Analysis. XLIII. Stereochemical Studies in the Cyclobutane Ring System1-3. *J Organ Chem*. 1965;30(6):1945–1951.
40 Vedejs E, Lin S. Deprotection of Arenesulfonamides with Samarium iodide. *J Organ Chem*. 1994;59(7):1602–1603.
41 Ankner T, Hilmersson G. Instantaneous Deprotection of Tosylamides and Esters with SmI2/Amine/Water. *Org Lett*. 2009;11(3):503–506.
42 Sabitha G, Reddy BVS, Abraham S, Yadav JS. Deprotection of sulfonamides using iodotrimethylsilane. *Tetrahedron Lett*. 1999;40(8):1569–1570.
43 Gethin DM, Simpkins NS. A new synthetic approach to the polyoxins: Concise stereoselective preparation of protected thymine polyoxin C. *Tetrahedron*. 1997;53(42):14417–14436.
44 Wang Q, Deredas D, Huynh C, Schlosser M. Sequestered Alkyllithiums: Why Phenyllithium Alone is Suitable for Betaine-Ylide Generation. *Chemistry – A. European Journal*. 2003;9(2):570–574.
45 Staab HA, Zipplies MF, Müller T, Storch M, Krieger C. Pyridinio-isoalloxazinophanes as Model Systems for Active-Site Complexes in Flavoenzymes: Syntheses, X-Ray Structure Analyses and Spectroscopic Properties. *Chemische Berichte*. 1994;127(9):1667–1680.
46 Maryanoff BE, Reitz AB. The Wittig olefination reaction and modifications involving phosphoryl-stabilized carbanions. Stereochemistry, mechanism, and selected synthetic aspects. *Chem Rev*. 1989;89(4):863–927.
47 Choudhary A, Raines RT. An evaluation of peptide-bond isosteres. *ChemBioChem*. 2011;12(12):1801–1807.
48 Bajorath J, Peltason L, Wawer M, Guha R, Lajiness MS, Van Drie JH. Navigating structure-activity landscapes. *Drug Discov Today*. 2009;14(13-14):698–705.
49 DataWarrior v05.02.01. http://www.openmolecules.org/index.html.
50 Guha R, Van Drie JH. Structure–activity landscape index: identifying and quantifying activity cliffs. *J Chem Inf Model*. 2008;48(3):646–658.
51 Molecular Operating Environment (MOE), 2019.0102; Chemical Computing Group ULC, 1010 Sherbrooke St. West, Suite #910, Montreal, QC, Canada, H3A 2R7, 2020.